

Chiral kinematic theory and converse vortical effects

Kai Chen, Swadeepan Nanda, and Pavan Hosur

Department of Physics and Texas Center for Superconductivity, University of Houston, Houston, TX 77204

(Dated: December 4, 2023)

Response theories in condensed matter typically describe the response of an electron fluid to external electromagnetic fields, while perturbations on neutral particles are often designed to mimic such fields. Here, we study the response of fermions to a space-time-dependent velocity field, thereby sidestepping the issue of a gauge charge. We first develop a semiclassical chiral kinematic theory that contains a subtle modification of the phase space measure due to interplay between the Berry curvature and fluid rotation. The theory immediately predicts a "converse vortical effect," defined as an orbital magnetization driven by linear velocity. It receives contributions from magnetic moments on the Fermi surface and Berry curvature of the occupied bands, with the latter stemming from the modified measure. Then, transcending semiclassics via a complementary Kubo formalism reveals that the uniform limit of a clean system receives only the Berry curvature contribution – thus asserting the importance of the modified measure – while other limits sense the Fermi surface magnetic moments too. We propose CoSi as a candidate material and magnetometry of a sample under a thermal gradient to detect the effect. Overall, our study sheds light on the effects of a space-time-dependent velocity field on electron fluids and paves the way for exploring quantum materials using new probes and perturbations.

Introduction.—Response theories, a fundamental framework in physics, explore how physical systems dynamically respond to external perturbations. In the context of quantum materials, they describe a myriad of properties ranging from conventional ones such as longitudinal conductivity and magnetization, to topological ones such as the quantized Hall conductivity of two-dimensional (2D) insulators and the half-quantum Hall effect on the surface of 3D topological insulators [1, 2]. As most responses involve the constituent electrons responding to external electromagnetic fields, response theories provide a bridge from microscopic quantum phenomena to macroscopic material properties and facilitate the design of novel functional materials tunable by these fields.

Since the discovery of Weyl semimetals (WSMs) [3–10], interest has mushroomed in chiral responses in condensed matter [11–16]. Chirality refers to an intrinsic handedness of the system and is non-zero only in systems that break all improper symmetries, such as an isolated Weyl fermion. Chiral responses were initially explored in various context in fundamental physics ranging from left-handed neutrinos [17, 18] and parity violation [19, 20] in the Standard Model to the fluid dynamics of rotating blackholes [21–24] and axion models of dark matter [25–27]. In WSMs, the basic chiral objects are band intersections or Weyl nodes which, at low energies, mimic massless, relativistic Weyl fermions. Most chiral responses can be traced to chiral anomalies, defined as the breakdown of classical conservation laws upon quantization of chiral fermion [16, 28–33]. The anomalies, too, were first explored in high-energy physics, but have found remarkable applications in topological condensed matter, particularly in Weyl and Dirac semimetals, manifesting as exotic transport phenomena [34–39].

A powerful framework that captures chiral responses is the chiral kinetic theory [40–49], a semiclassical description of the electromagnetic responses of general chiral fermions. A key feature of the theory that

encodes the topological content of various responses is the enhancement of the phase space measure in the n -th band by $1 + \mathbf{B} \cdot \boldsymbol{\Omega}_n(\mathbf{k})$, where \mathbf{B} is the magnetic field and $\boldsymbol{\Omega}_n(\mathbf{k})$ is the Berry curvature of the band and momentum \mathbf{k} . Using analogies between electromagnetic and fictitious non-inertial fields, such as the similarity between the classical Lorentz and Coriolis forces, chiral kinetic theory can also encompass certain responses of Weyl fermions to space and time-dependent velocity fields $\mathbf{v}(\mathbf{r}, t)$ [43, 50? –54]. Such kinematic responses are routinely used to simulate gauge fields for neutral ultracold atoms [55–58]. They are arguably more fundamental than electromagnetic responses as they do not rely on a well-defined conserved charge and exist, for instance, even for superconducting quasiparticles whose charge is ill-defined. However, while the analogies are established for non-relativistic and relativistic free particles in vacuum, they are unknown for electrons in general band structures. Thus, a general description of kinematic responses independently of electromagnetic analogies is highly desirable.

In this work, we first derive a semiclassical chiral kinematic theory (CKmT) that delineates the linear response of electrons in general band structures to $\mathbf{v}(\mathbf{r}, t)$. In particular, we show that fluid vorticity or local angular velocity, $\boldsymbol{\mathcal{V}} = \frac{1}{2} \boldsymbol{\nabla} \times \mathbf{v}$, alters the semiclassical equations of motion in a way that forces a modification of the phase space measure to conserve the phase space Liouvillian density. The modification affects thermodynamic quantities such as free energy and immediately predicts an orbital magnetization

$$\mathbf{M}^{\text{orb}} = \chi \mathbf{v} \quad (1)$$

that we term the converse vortical effect. Classically, the converse vortical effect can be explained using the analogy of a screw. When a screw is rotated faster, it generates more torque, which transforms into a linear force, allowing the screw to move faster along its axis. This circular rotation induces linear motion, corresponding to the vortical effect. Conversely, when a screw has a higher

linear speed, it drills into objects with a greater circular rotation. This linear motion induces a converse vortical effect in the form of circular rotation.

The converse vortical effect is governed by two crucial factors: the orbital magnetic moment $\mathbf{m}_n^{\text{orb}}(\mathbf{k})$ on the Fermi surface and $\Omega_n(\mathbf{k})$ of occupied bands, the latter stemming from the modified phase space measure. A similar separation of contributions occurs in modern theories of orbital magnetization based on semiclassical wavepacket dynamics [59–64] or quantum perturbation theory [65] in electromagnetic fields. However, we stress that the CKmT, despite sharing similarities with established chiral kinetic theories of electromagnetic response [40, 41, 43, 66], is derived here using suitable approximations rather than analogies, which makes it useful for general band structures. For instance, we introduce an effective mass tensor \mathfrak{M}_n that captures the strength of the coupling between \mathbf{V} and $\Omega_n(\mathbf{k})$, playing a similar role as the electric charge in chiral kinetic theory.

We then employ a complementary, quantum mechanical Kubo approach to compute the linear response function at general frequencies ω and momenta \mathbf{q} of the velocity field in the presence of a phenomenological quasiparticle lifetime τ . This approach shows that the uniform limit of a clean system, defined by $q = 0$, $\omega \rightarrow 0$ and $|\omega\tau| \gg 1$, has a response purely governed by $\Omega_n(\mathbf{k})$ of the occupied bands that reduces to the contribution from the modified phase space measure in the semiclassical limit. In contrast, other orders of limits of $\omega \rightarrow 0$, $q \rightarrow 0$ and $\tau \rightarrow \infty$ also acquire contributions from $\mathbf{m}_n^{\text{orb}}(\mathbf{k})$ on the Fermi surface. We refer to the response in the uniform limit ($q \rightarrow 0$ before $\omega \rightarrow 0$) as the converse gyrotropic vortical effect (cGVE), and that in the static limit ($q \rightarrow 0$ after $\omega \rightarrow 0$) as the converse chiral vortical effect (cCVE).

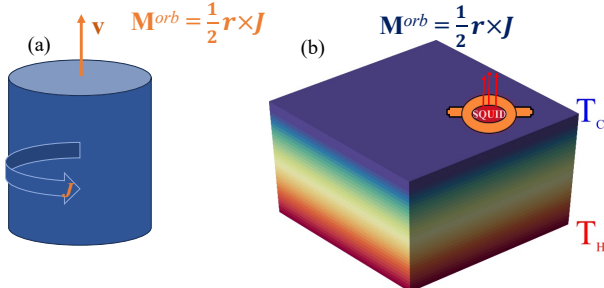


FIG. 1. Color online. (a) Schematic depiction of the converse vortical effect. (b) Device geometry for observing the converse vortical effect: The temperature difference propels electrons, inducing their motion with velocity \mathbf{v} . The resulting magnetization can be observed aligned with the velocity field.

To understand the converse effects – and their nomenclature – in a broader context, let us recap other closely related effects. First, continuum Weyl fermions in a \mathbf{B} -field exhibit the chiral magnetic effect (CME), arising from the chiral anomaly and manifesting as a current parallel to \mathbf{B} [3, 4, 12], unlike conventional charged particles that undergo circular motion in an

orthogonal plane. In WSMs, the CME vanishes at equilibrium due to lattice regularization but persists in non-equilibrium steady states with unequal Fermi levels for left- and right-handed Weyl nodes. Reconciling the continuum and lattice manifestations of the CME involved considering non-zero \mathbf{q} and ω responses. The original CME emerges in the static limit and relies on the existence of Weyl nodes while the uniform limit revealed a new effect, termed the gyrotropic magnetic effect (GME) [13, 66], that corresponds to a current along a time-dependent \mathbf{B} -field and exists for general band structures. Analogous to the CME, the chiral vortical effect (CVE) corresponds to the static limit and represents another anomaly-induced transport phenomenon [53, 54, 67–72], namely, the dissipationless axial current proportional to $\mathbf{V} = \frac{1}{2}\nabla \times \mathbf{v}$. Similarly, the gyrotropic vortical effect (GVE) was recently defined as the extension of the CVE to the uniform limit that crucially relies on the time-dependence of \mathbf{V} [50]. Both vortical effects exist at equilibrium for general band structures regardless of Weyl nodes. In short, the CME and GME are defined by $\mathbf{J} \propto \mathbf{B}$ in different limits whereas the CVE and GVE are given by $\mathbf{J} \propto \mathbf{V}$ in these limits.

The GME inspires an effect dubbed the inverse GME, defined as magnetization proportional to the vector potential, $\mathbf{M} \propto \mathbf{A}$ with a response function that is the matrix inverse of that of the GME [66]. The CME lacks an inverse response since a static \mathbf{A} is a pure gauge field. The GME and its inverse are related by an interchange of conjugate variables, $\mathbf{J} \leftrightarrow \mathbf{A}$ and $\mathbf{B} \leftrightarrow \mathbf{M}$, followed by an interchange of the left- and right-hand sides. Physically, this means the field \mathbf{A} conjugate to the GME response \mathbf{J} drives the inverse GME, and vice versa. This pattern suggests analogous inverse kinematic responses where a linear momentum \mathbf{P} , conjugate to the linear current or velocity \mathbf{J} or \mathbf{v} , drives an angular momentum \mathbf{L} that is conjugate to the angular velocity \mathbf{V} . While such responses presumably exist, our focus is on a distinct class of effects: unlike the inverse effects, the converse effects correspond to an interchange of responding and driving fields without conjugation. Thus, we wish to compute an angular velocity \mathbf{V} driven by a linear velocity \mathbf{v} . However, we compute a slightly different quantity that also characterizes rotational motion, namely, $\mathbf{M}^{\text{orb}} \equiv \frac{1}{2}\mathbf{r} \times \mathbf{J}$ as a proxy for \mathbf{V} , as \mathbf{M}^{orb} is directly measurable in experiments and easier to compute than \mathbf{V} . Note that \mathbf{L} , not \mathbf{M}^{orb} , is conjugate to \mathbf{V} , even though $\mathbf{L} \propto \mathbf{M}^{\text{orb}}$ in simple cases such as a classical current loop.

Chiral kinematic theory.—Consider lattice fermions obeying the Bloch Hamiltonian $H_0(\mathbf{k})$ driven by a velocity field $\mathbf{v}(\mathbf{r}, t)$ that is much smaller than typical band velocities. In the continuum limit, the full Hamiltonian can be written as $H_0(\mathbf{k}) - \mathbf{k} \cdot \mathbf{v}(\mathbf{r}, t)$. Similar to \mathbf{B} in the chiral kinetic theory, we derive in Appendix A that \mathbf{V} modifies the phase space measure in the free energy

density:

$$F = -\frac{1}{\beta} \sum_n \int_{\mathbf{k}} (1 + 2\Omega_n(\mathbf{k}) \cdot \mathfrak{M}_n \cdot \mathbf{V}) \times \ln \left(1 + e^{-\beta(\epsilon_{n,\mathbf{k}} - \mathbf{k} \cdot \mathbf{v} - 2\mathbf{m}_n^{\text{orb}}(\mathbf{k}) \cdot \mathfrak{M}_n \cdot \mathbf{V})} \right) \quad (2)$$

where $\int_{\mathbf{k}} \equiv \int \frac{d^3 k}{(2\pi)^3}$, β is the inverse temperature, $\mathbf{m}_n^{\text{orb}}(\mathbf{k}) \equiv \frac{i}{2} \langle \nabla_{\mathbf{k}} u_{n,\mathbf{k}} \rangle \times (\epsilon_{n,\mathbf{k}} - H_0(\mathbf{k})) \langle \nabla_{\mathbf{k}} u_{n,\mathbf{k}} \rangle$, $\Omega_n(\mathbf{k}) \equiv i \langle [\nabla_{\mathbf{k}} u_{n,\mathbf{k}}] \times [\nabla_{\mathbf{k}} u_{n,\mathbf{k}}] \rangle$, and the mass-like tensor \mathfrak{M}_n is defined by the equation:

$$-\mathbf{k} \cdot \mathbf{v} = \frac{1}{2} \left\{ \frac{\partial H_0(\mathbf{k})}{\partial \mathbf{k}}, \mathfrak{M}_n \cdot \mathbf{v} \right\} \quad (3)$$

where $\{, \}$ denotes an anticommutative operation. While \mathfrak{M}_n reduces, upto a sign, to the effective mass based on band curvature for simple parabolic dispersions, it is distinct in general. For instance, a Weyl fermion with unperturbed Hamiltonian $H_0(\mathbf{k}) = \mathbf{k} \cdot \boldsymbol{\sigma}$ has $\mathfrak{M}_n = -\sigma_z \mathbf{k}$, in agreement with Ref. [43].

The derivation of \mathfrak{M}_n and the measure in Eq. (2) for the free energy density represents a significant outcome of this study. This measure can be obtained from the equations governing the semiclassical motion which are denoted as:

$$\begin{aligned} \dot{\mathbf{r}} &= \partial_{\mathbf{k}} h_n - \dot{\mathbf{k}} \times \Omega_n(\mathbf{k}), \\ \dot{\mathbf{k}} &= -\partial_{\mathbf{r}} h_n - \dot{\mathbf{r}} \times 2\mathfrak{M}_n \cdot \mathbf{V}, \end{aligned} \quad (4)$$

where $h_n = \epsilon_{n,\mathbf{k}} - \mathbf{k} \cdot \mathbf{v} - 2\mathbf{m}_n^{\text{orb}} \cdot \mathfrak{M}_n \cdot \mathbf{V}$. If \mathfrak{M}_n were constant, as it would be for a parabolic dispersion, the term $\dot{\mathbf{r}} \times 2\mathfrak{M}_n \cdot \mathbf{V}$ in Eq. (4) would reduce to the Coriolis force while $2\mathbf{m}_n^{\text{orb}} \cdot \mathfrak{M}_n \cdot \mathbf{V}$ would be a magneto-vortical coupling. In either case, the term $2\mathfrak{M}_n \cdot \mathbf{V}$ plays the role of an effective magnetic field. Thus, Eq. (4) and h_n can be understood as generalizations of these effects for arbitrary bands.

In canonical coordinates (\mathbf{x}, \mathbf{p}) , the familiar Hamiltonian pair $\dot{\mathbf{x}} = \partial_{\mathbf{p}} h_n$ and $\dot{\mathbf{p}} = -\partial_{\mathbf{x}} h_n$ holds. However, the presence of terms related to the Berry curvature and the angular velocity in Eq. (4) suggests that the coordinates (\mathbf{r}, \mathbf{k}) are noncanonical[73–77]. Consequently, the phase-space volume element $dV \equiv d^3 x d^3 p$ is modified to $dV = (1 + 2\Omega_n \cdot \mathfrak{M}_n \cdot \mathbf{V}) d^3 r d^3 k$. Consider a probability distribution function over the phase space volume, denoted as $n(\mathbf{r}, \mathbf{k}, t)(1 + 2\Omega_n \cdot \mathfrak{M}_n \cdot \mathbf{V}) d\mathbf{r} d\mathbf{k}$. Under a Hamiltonian flow (without collisions), it evolves according to

$$\frac{\partial n}{\partial t} + \partial_{\mathbf{r}}(n\dot{\mathbf{r}}) + \partial_{\mathbf{k}}(n\dot{\mathbf{k}}) = -n \frac{d_t(2\Omega_n \cdot \mathfrak{M}_n \cdot \mathbf{V})}{1 + 2\Omega_n \cdot \mathfrak{M}_n \cdot \mathbf{V}}, \quad (5)$$

where $d_t(2\Omega_n \cdot \mathfrak{M}_n \cdot \mathbf{V}) \equiv \partial_{\mathbf{r}}(2\Omega_n \cdot \mathfrak{M}_n \cdot \mathbf{V}) \cdot \dot{\mathbf{r}} + \partial_{\mathbf{k}}(2\Omega_n \cdot \mathfrak{M}_n \cdot \mathbf{V}) \cdot \dot{\mathbf{k}}$. This equation does not have a form of the continuity relation, due to the presence of the right-hand side. This reflects the fact that $\int d\mathbf{r} d\mathbf{k} n(\mathbf{r}, \mathbf{k}, t)$ is not conserved. However, the quantity $\int d\mathbf{r} d\mathbf{k} \rho(\mathbf{r}, \mathbf{k}, t) \equiv \int d\mathbf{r} d\mathbf{k} n(\mathbf{r}, \mathbf{k}, t)(1 + 2\Omega_n \cdot \mathfrak{M}_n \cdot \mathbf{V})$ remains conserved.

Therefore, any observables should be expressed as $O_t = \int d\mathbf{r} d\mathbf{k} (1 + 2\Omega_n \cdot \mathfrak{M}_n \cdot \mathbf{V}) n(\mathbf{r}, \mathbf{k}, t) O(\mathbf{r}, \mathbf{k}, t)$.

The converse vortical effect refers to the response of orbital magnetization to velocity. In order to calculate the density of orbital magnetization, we differentiate the free energy density with respect to $2\mathfrak{M}_n \cdot \mathbf{V}$ while keeping the temperature $T = \beta^{-1}$ fixed. This calculation leads to:

$$\begin{aligned} \mathbf{M}^{\text{orb}}(\mathbf{v}) &= -\frac{\delta F}{\delta(2\mathfrak{M}_n \cdot \mathbf{V})}_{|T, \mathbf{V}=0} \\ &= \sum_n \int_{\mathbf{k}} \mathbf{m}_n^{\text{orb}}(\mathbf{k}) f(\epsilon_{n,\mathbf{k}}, \mathbf{v}) \\ &\quad + \frac{1}{\beta} \int_{\mathbf{k}} \Omega_n(\mathbf{k}) \ln \left(1 + e^{-\beta(\epsilon_{n,\mathbf{k}} - \mathbf{k} \cdot \mathbf{v})} \right) \\ &\equiv \chi^{\text{orb}} \cdot \mathbf{v} + O(\mathbf{v}^2) \end{aligned} \quad (6)$$

where Fermi distribution function $f(\epsilon_{n,\mathbf{k}}, \mathbf{v}) \equiv (e^{\beta(\epsilon_{n,\mathbf{k}} - \mathbf{k} \cdot \mathbf{v})} + 1)^{-1}$, and the tensor χ^{orb} representing the orbital magnetic susceptibility is denoted as:

$$\begin{aligned} \chi_{ij}^{\text{orb}} &= -\sum_n \int_{\mathbf{k}} m_{n,i}^{\text{orb}}(\mathbf{k}) f'(\epsilon_{n,\mathbf{k}}) k_j \\ &\quad + \sum_n \int_{\mathbf{k}} f(\epsilon_{n,\mathbf{k}}) \Omega_{n,i}(\mathbf{k}) k_j \equiv \chi_{ij}^{\text{Fs}} + \chi_{ij}^{\text{occ}} \end{aligned} \quad (7)$$

The equation above reveals that the magnetic susceptibility is determined by the orbital magnetic moment of electrons on the Fermi surface (indicated as χ_{ij}^{Fs}) as well as the Berry curvature of the occupied bands (indicated as χ_{ij}^{occ}). Interestingly, this response function takes the same form as the vortical effect[50]. However, they represent distinct responses. In the vortical effect, the response function denotes the axial current response to angular velocity, while in the converse vortical effect, the response function represents the orbital magnetization response to velocity.

Converse vortical effect for general band structures.— In this section, we employ the Kubo formula to compute χ_{ij}^{orb} at general \mathbf{q} and ω in the presence of quasiparticle lifetime τ . The Bloch energy and wave function for the n -th band are given by $\epsilon_{n,\mathbf{k}}$ and $\psi_{n,\mathbf{k}}(\mathbf{r}) = \psi_{n,\mathbf{k}}(\mathbf{R} + \boldsymbol{\rho}) = N^{-1/2} e^{i\mathbf{k} \cdot (\mathbf{R} + \boldsymbol{\rho})} u_{n,\mathbf{k}}(\boldsymbol{\rho})$, respectively, where \mathbf{R} denotes the coordinates of the unit cells, $\boldsymbol{\rho}$ represents position within each unit cell and N is the total number of unit cells. In this basis, the matrix elements of the velocity-induced perturbation $H_1 = -\hat{\mathbf{p}} \cdot \mathbf{v}(\mathbf{r}, t)$ with $\hat{\mathbf{p}}$ denoting the momentum operator, are $\langle \psi_{n,\mathbf{k}} | H_1 | \psi_{m,\mathbf{k}+\mathbf{p}} \rangle = (2\pi)^3 \langle u_{n,\mathbf{k}} | (\mathbf{k} - i\nabla_{\boldsymbol{\rho}}) | u_{m,\mathbf{k}+\mathbf{p}} \rangle \cdot \mathbf{v}(\mathbf{p}, t)$, where $\mathbf{v}(\mathbf{p}, t)$ is $\mathbf{v}(\mathbf{r}, t)$ Fourier transformed to momentum space. Thus, it is convenient to introduce the operator $\hat{\mathbf{Q}} = \mathbf{k} - i\nabla_{\boldsymbol{\rho}}$ and write $H_1 = -\hat{\mathbf{Q}} \cdot \mathbf{v}$. Unlike the continuum perturbation $-\mathbf{k} \cdot \mathbf{v}$, H_1 respects the Brillouin Zone periodicity and can be viewed as the kinematic analog of minimal coupling $\mathbf{J} \cdot \mathbf{A}$ that is well-defined on a lattice through Peierls's substitution [50].

To calculate χ_{ij}^{orb} , we Fourier transform $\mathbf{M}^{\text{orb}} = \frac{1}{2} \mathbf{r} \times \mathbf{J}$ to Bloch momentum and Matsubara frequencies,

Limit	Definition	χ_{ij}^{occ}	χ_{ij}^{Fs}	$\chi_{ij}^{\text{Weyl}} = \chi_{ij}^{\text{occ}} + \chi_{ij}^{\text{Fs}}$
Uniform, clean	$ \nabla_{\mathbf{k}}\epsilon_{n,\mathbf{k}} \cdot \mathbf{q}\tau \ll \omega , \omega\tau \gg 1$	$\sum_n \int_{\mathbf{k}} \Omega_{n,i}(\mathbf{k}) \Theta(-\epsilon_{n,\mathbf{k}}) k_j$	0	$\frac{1}{6}\chi_{ij}^{\mathcal{C}} = \frac{1}{6}\chi_{ij}^{\mathcal{C}} + 0$
Static, clean	$ \nabla_{\mathbf{k}}\epsilon_{n,\mathbf{k}} \cdot \mathbf{q}\tau \gg \omega , v_F q\tau \gg 1$	$\sum_n \int_{\mathbf{k}} \Omega_{n,i}(\mathbf{k}) \Theta(-\epsilon_{n,\mathbf{k}}) k_j$	$\sum_n \int_{\mathbf{k}} m_{n,i}^{\text{orb}}(\mathbf{k}) \delta(\epsilon_{n,\mathbf{k}}) k_j$	$\frac{1}{2}\chi_{ij}^{\mathcal{C}} = \frac{1}{3}\chi_{ij}^{\mathcal{C}} + \frac{1}{6}\chi_{ij}^{\mathcal{C}}$
Uniform, disorder	$ \nabla_{\mathbf{k}}\epsilon_{n,\mathbf{k}} \cdot \mathbf{q}\tau \ll \omega , \omega\tau \ll 1$	$\sum_n \int_{\mathbf{k}} \Omega_{n,i}(\mathbf{k}) \Theta(-\epsilon_{n,\mathbf{k}}) k_j$	$\sum_n \int_{\mathbf{k}} m_{n,i}^{\text{orb}}(\mathbf{k}) \delta(\epsilon_{n,\mathbf{k}}) k_j$	$\frac{1}{2}\chi_{ij}^{\mathcal{C}} = \frac{1}{3}\chi_{ij}^{\mathcal{C}} + \frac{1}{6}\chi_{ij}^{\mathcal{C}}$
Static, disorder	$ \nabla_{\mathbf{k}}\epsilon_{n,\mathbf{k}} \cdot \mathbf{q}\tau \gg \omega , v_F q\tau \ll 1$	$\sum_n \int_{\mathbf{k}} \Omega_{n,i}(\mathbf{k}) \Theta(-\epsilon_{n,\mathbf{k}}) k_j$	$\sum_n \int_{\mathbf{k}} m_{n,i}^{\text{orb}}(\mathbf{k}) \delta(\epsilon_{n,\mathbf{k}}) k_j$	$\frac{1}{2}\chi_{ij}^{\mathcal{C}} = \frac{1}{3}\chi_{ij}^{\mathcal{C}} + \frac{1}{6}\chi_{ij}^{\mathcal{C}}$

TABLE I. Summary of results as $q \rightarrow 0$ and $\omega \rightarrow 0$ at various orders is presented for general band structures. The last column represents the orbital magnetization for an isotropic Weyl fermion with a velocity of v_F , chiral charge \mathcal{C} , and chemical potential μ relative to the Weyl node. Here, $\chi_{ij}^{\mathcal{C}} = \mathcal{C} \left(\frac{\mu}{2\pi v_F} \right)^2 \delta_{ij}$.

$\mathbf{M}^{\text{orb}}(\mathbf{q}, iq_n) = \frac{i}{2} \nabla_{\mathbf{q}} \times \mathbf{J}(\mathbf{q}, iq_n)$, and compute the susceptibility, $\chi_{ij}^{\text{orb}}(\mathbf{q}, iq_n) = \frac{\partial M_i^{\text{orb}}}{\partial v_j}(\mathbf{q}, iq_n)$ with i and j denoting spatial components. The basic one-loop diagram yields

$$\chi_{ij}^{\text{orb}}(\mathbf{q}, iq_n) = -\epsilon_{i\mu\nu} i\partial_{q_\mu} \frac{1}{2\beta} \sum_{i\nu_n} \int_{\mathbf{k}} \text{tr} [j_\nu(\mathbf{k} + \mathbf{q}) G_0(\mathbf{k}, i\nu_n) G_0(\mathbf{k} + \mathbf{q}, i\nu_n + iq_n) Q_j] \quad (8)$$

where $G_0(\mathbf{k}, i\nu_n) = [i\nu_n - H_0(\mathbf{k}) + i\text{sgn}(\nu_n)/2\tau]^{-1}$ is the unperturbed Matsubara Green's function, the elements of the matrix Q_j are $Q_j^{mn} = \langle u_{m,\mathbf{k}} | \hat{Q}_j | u_{n,\mathbf{k}+\mathbf{q}} \rangle$, $j_\nu(\mathbf{k}) = \frac{\partial H_0(\mathbf{k})}{\partial k_\nu}$ is the current density operator and repeated indices are summed. The retarded response function follows from analytically continuing $iq_n \rightarrow \omega + i0^+$. The Matsubara sum yields

$$\chi_{ij}^{\text{orb}}(\mathbf{q}, iq_n) = -\frac{1}{2} \epsilon_{i\mu\nu} i\partial_{q_\mu} \int_{\mathbf{k}} \sum_{n,m} S_{m,n}(\mathbf{k}, \mathbf{q}, iq_n) \langle u_{n,\mathbf{k}+\mathbf{q}} | j_\nu(\mathbf{k} + \mathbf{q}) | u_{m,\mathbf{k}} \rangle Q_j^{mn}, \quad (9)$$

where

$$S_{m,n}(\mathbf{k}, \mathbf{q}, iq_n) = \frac{1}{\beta} \sum_{i\nu_n} \frac{1}{i\nu_n - \epsilon_{m,\mathbf{k}} + i\frac{\text{sgn}(\nu_n)}{2\tau}} \frac{1}{i\nu_n + iq_n - \epsilon_{n,\mathbf{k}+\mathbf{q}} + i\frac{\text{sgn}(\nu_n+q_n)}{2\tau}}. \quad (10)$$

At zero temperature, the off-diagonal elements of the matrix Q_j couple to the inter-band orbital magnetization matrix of the Bloch electrons [78], contributing to the orbital magnetization (for more details, see the Supplemental Material). In this section, we explore the zero-temperature regime in the context of both the nearly-free electron approximation and the deep tight-binding approximation [50]. Under these conditions, the Fermi distribution function $f(\epsilon_{n\mathbf{k}})$ and Q_j^{mn} simplify to $\Theta(-\epsilon_{n\mathbf{k}})$ and $k_j \delta_{mn}$, respectively. The difference between various orders of limits of $\omega \rightarrow 0$, $q \rightarrow 0$ and $\tau \rightarrow \infty$ is determined by the behavior of $S_{m,n}$ in these limits. In the static limit ($\omega \rightarrow 0$ followed by $q \rightarrow 0$), we find χ_{ij}^{orb} reduces to Eq. (7) derived using CKmT for both $v_F q\tau \gg 1$ and $v_F q\tau \ll 1$,

where v_F is a typical band velocity. In contrast, the dirty uniform limit, ($\mathbf{q} \rightarrow 0$ followed by $\omega \rightarrow 0$ with $|\omega\tau| \ll 1$), leads to Eq. (7) while the clean uniform limit ($\mathbf{q} \rightarrow 0$ followed by $\omega \rightarrow 0$ with $|\omega\tau| \gg 1$) gives:

$$\chi_{ij}^{\text{orb}} = \int_{\mathbf{k}} \sum_n \Theta(-\epsilon_{n,\mathbf{k}}) \Omega_{n,i}(\mathbf{k}) k_j \quad (11)$$

Thus, χ_{ij}^{orb} in this limit is solely determined by $\Omega_n(\mathbf{k})$ of occupied bands. It is worth noting that the $\Omega_n(\mathbf{k})$ contribution vanishes for a filled band in the continuum limit at zero temperature, where $\hat{Q}_j \rightarrow \hat{k}_j$ and $u_{n,\mathbf{k}}$ become \mathbf{k} -independent as $k \rightarrow \infty$, similarly to the GVE [50]. Therefore, only partially filled bands contribute to \mathbf{M}^{orb} in any limit. The results are summarized in Table I. However, in a disordered electron fluid, both the Berry curvature of the occupied bands and the orbital moment of electrons on the Fermi surface contribute to the magnetic susceptibility in both the static and uniform limits. This magnetic susceptibility takes the same form as described in Eq. (7), acquiring the combined effects of the Berry curvature and the orbital moment.

cCVE and cGVE of Weyl fermions.—We now evaluate χ_{ij}^{orb} for a single, isotropic, continuum Weyl fermion with chirality $\mathcal{C} = \pm 1$. The effective Hamiltonian is given by $H(\mathbf{k}) = \mathcal{C} \mathbf{k} \cdot \boldsymbol{\sigma} - \mu - \mathbf{k} \cdot \mathbf{v}$, where $\boldsymbol{\sigma}$ represents the Pauli matrices and μ is the chemical potential relative to the Weyl node and \mathbf{v} . The results at $T = 0$ are stated in Table I. Since the effect is proportional to the chirality \mathcal{C} and μ^2 , improper symmetries must be broken for a material with pairs of Weyl fermions to show an effect as improper symmetries reverse \mathcal{C} while preserving μ .

To experimentally observe the converse vortical effects, we propose a simple experiment sketched in Fig. 1. This is significantly simpler than the curved geometries required for the vortical effects [50]. By leveraging a temperature difference gradient ($\nabla T \approx 1K/\mu\text{m}$) and a Seebeck coefficient ($S = 100a\mu\text{V}/K$), we generate an electric field strength of $|\mathbf{E}| = 0.1\text{V}/\text{m}$, driving the motion of electrons relative to the lattice. Consequently, \mathbf{M}^{orb} aligns with $\mathbf{v} = \mu_{\text{mob}} \mathbf{E}$, with μ_{mob} representing the mobility of the system. For a WSM with typical parameter values such as $\mu_{\text{mob}} = 10^5 \text{cm}^2/(\text{Vs})$, $v_F = 10^5 \text{m/s}$, and Fermi energy differences $\mu_{\pm} = (0.5 \pm 0.025) \text{eV}$ relative to the left-handed/right-handed Weyl nodes, $|\mathbf{M}^{\text{orb}}| \approx 4.68 \times 10^{-2} \text{A/m}$. Moreover, Weyl nodes are

not mandatory, and the converse vortical effects can also occur in a chiral semimetal such as CoSi [79–81].

Summary.—We employ semiclassical wave-packet dynamics to develop a chiral kinematic theory for investigating the influence of space-time-dependent velocity fields on electron fluids. By analyzing the modified free energy density, we explore the orbital magnetization response, known as the converse vortical effect, induced by the velocity field. Through the application of the Kubo formula, we calculate the converse vortical effect under different limits. Our study reveals that the magnetic susceptibility in the static limit, which encompasses both clean and disordered systems, and in the uniform limit of disordered systems, is primarily governed by the orbital moment on the Fermi surface and the Berry curvature of occupied bands. These findings are in agreement with the predictions derived from chiral kinematic theories. However, in the uniform limit of clean systems, a significant deviation from the predictions of the chiral kinematic theory is observed. In this regime, the susceptibility is solely determined by the Berry curvature of occupied bands. This research provides valuable insights into the behavior of electron fluids under space-time-dependent velocity fields, shedding light on the intricate relationship between the velocity field and electron properties. Our results contribute to advancing the understanding of fundamental physical phenomena and offer opportunities for exploring new applications in electron fluid systems.

We acknowledge support from the Department of Energy grant no. DE-SC0022264.

[1] M. Z. Hasan and C. L. Kane, *Reviews of modern physics* **82**, 3045 (2010).

[2] X.-L. Qi and S.-C. Zhang, *Reviews of Modern Physics* **83**, 1057 (2011).

[3] N. Armitage, E. Mele, and A. Vishwanath, *Reviews of Modern Physics* **90**, 015001 (2018).

[4] P. Hosur and X. Qi, *Comptes Rendus Physique* **14**, 857 (2013).

[5] X. Wan, A. M. Turner, A. Vishwanath, and S. Y. Savrasov, *Physical Review B* **83**, 205101 (2011).

[6] A. Burkov and L. Balents, *Physical review letters* **107**, 127205 (2011).

[7] B. Lv, H. Weng, B. Fu, X. P. Wang, H. Miao, J. Ma, P. Richard, X. Huang, L. Zhao, G. Chen, *et al.*, *Physical Review X* **5**, 031013 (2015).

[8] A. A. Soluyanov, D. Gresch, Z. Wang, Q. Wu, M. Troyer, X. Dai, and B. A. Bernevig, *Nature* **527**, 495 (2015).

[9] H. Weng, C. Fang, Z. Fang, B. A. Bernevig, and X. Dai, *Physical Review X* **5**, 011029 (2015).

[10] S.-Y. Xu, I. Belopolski, N. Alidoust, M. Neupane, G. Bian, C. Zhang, R. Sankar, G. Chang, Z. Yuan, C.-C. Lee, *et al.*, *Science* **349**, 613 (2015).

[11] A. Zyuzin and A. Burkov, *Physical Review B* **86**, 115133 (2012).

[12] Q. Li, D. E. Kharzeev, C. Zhang, Y. Huang, I. Pletikosić, A. Fedorov, R. Zhong, J. Schneeloch, G. Gu, and T. Valla, *Nature Physics* **12**, 550 (2016).

[13] J. Ma and D. Pesin, *Physical Review B* **92**, 235205 (2015).

[14] Z.-M. Huang, J. Zhou, and S.-Q. Shen, *Physical Review B* **96**, 085201 (2017).

[15] N. Ong and S. Liang, *Nature Reviews Physics* **3**, 394 (2021).

[16] S. Jia, S.-Y. Xu, and M. Z. Hasan, *Nature materials* **15**, 1140 (2016).

[17] T. Yanagida, *Progress of Theoretical Physics* **64**, 1103 (1980).

[18] G. B. Gelmini and M. Roncadelli, *Physics Letters B* **99**, 411 (1981).

[19] T.-D. Lee and C.-N. Yang, *Physical Review* **104**, 254 (1956).

[20] C.-S. Wu, E. Ambler, R. W. Hayward, D. D. Hoppes, and R. P. Hudson, *Physical review* **105**, 1413 (1957).

[21] A. Vilenkin, *Physical Review D* **20**, 1807 (1979).

[22] N. Yamamoto, *Physical Review D* **93**, 065017 (2016).

[23] G. Y. Prokhorov, O. Teryaev, and V. Zakharov, *Physical Review D* **102**, 121702 (2020).

[24] A. Flachi and K. Fukushima, *Physical Review D* **98**, 096011 (2018).

[25] S. Alexander, E. McDonough, and D. N. Spergel, *Journal of Cosmology and Astroparticle Physics* **2018** (05), 003.

[26] L. Di Luzio, G. Martinelli, and G. Piazza, *Physical review letters* **126**, 241801 (2021).

[27] F. Chadha-Day, J. Ellis, and D. J. Marsh, *Science advances* **8**, eabj3618 (2022).

[28] S. L. Adler, *Physical Review* **177**, 2426 (1969).

[29] B. Zumino, W. Yong-Shi, and A. Zee, *Nuclear Physics B* **239**, 477 (1984).

[30] A. Y. Alekseev, V. V. Cheianov, and J. Fröhlich, *Physical review letters* **81**, 3503 (1998).

[31] C.-L. Zhang, S.-Y. Xu, I. Belopolski, Z. Yuan, Z. Lin, B. Tong, G. Bian, N. Alidoust, C.-C. Lee, S.-M. Huang, *et al.*, *Nature communications* **7**, 1 (2016).

[32] N. Mueller and R. Venugopalan, *Physical Review D* **97**, 051901 (2018).

[33] C. Rylands, A. Parhizkar, A. A. Burkov, and V. Galitski, *Physical Review Letters* **126**, 185303 (2021).

[34] E. Gorbar, V. Miransky, and I. Shovkovy, *Physical Review B* **89**, 085126 (2014).

[35] A. C. Potter, I. Kimchi, and A. Vishwanath, *Nature communications* **5**, 5161 (2014).

[36] J. Xiong, S. K. Kushwaha, T. Liang, J. W. Krizan, M. Hirschberger, W. Wang, R. J. Cava, and N. P. Ong, *Science* **350**, 413 (2015).

[37] A. G. Grushin, J. W. Venderbos, A. Vishwanath, and R. Ilan, *Physical Review X* **6**, 041046 (2016).

[38] A. Burkov, *Nature materials* **15**, 1145 (2016).

[39] T. Liang, J. Lin, Q. Gibson, T. Gao, M. Hirschberger, M. Liu, R. J. Cava, and N. P. Ong, *Physical review letters* **118**, 136601 (2017).

[40] D. T. Son and N. Yamamoto, *Physical review letters* **109**, 181602 (2012).

[41] D. Son and B. Spivak, *Physical Review B* **88**, 104412 (2013).

[42] D. T. Son and N. Yamamoto, *Physical review D* **87**, 085016 (2013).

[43] M. Stephanov and Y. Yin, *Physical review letters* **109**, 162001 (2012).

[44] A. Burkov, *Journal of Physics: Condensed Matter* **27**, 113201 (2015).

[45] Y.-C. Liu, L.-L. Gao, K. Mameda, and X.-G. Huang, *Physical Review D* **99**, 085014 (2019).

[46] D. Kharzeev, J. Liao, S. Voloshin, and G. Wang, *Progress in Particle and Nuclear Physics* **88**, 1 (2016).

[47] J.-W. Chen, T. Ishii, S. Pu, and N. Yamamoto, *Physical Review D* **93**, 125023 (2016).

[48] Y. Hidaka, S. Pu, and D.-L. Yang, *Physical Review D* **97**, 016004 (2018).

[49] K. Mameda, arXiv preprint arXiv:2305.02134 (2023).

[50] S. Nanda and P. Hosur, *Physical Review B* **107**, 205107 (2023).

[51] Ö. F. Dayi and E. Kilinçarslan, *Physical Review D* **98**, 081701 (2018).

[52] Ö. F. Dayi and E. Kilinçarslan, *Journal of High Energy Physics* **2021**, 1 (2021).

[53] A. Shitade, K. Mameda, and T. Hayata, *Physical Review B* **102**, 205201 (2020).

[54] R. Toshio, K. Takasan, and N. Kawakami, *Physical Review Research* **2**, 032021 (2020).

[55] N. R. Cooper, *Advances in Physics* **57**, 539 (2008).

[56] Y.-J. Lin, R. L. Compton, K. Jiménez-García, J. V. Porto, and I. B. Spielman, *Nature* **462**, 628 (2009).

[57] A. L. Fetter, *Reviews of Modern Physics* **81**, 647 (2009).

[58] N. Goldman, G. Juzeliūnas, P. Öhberg, and I. B. Spielman, *Reports on Progress in Physics* **77**, 126401 (2014).

[59] G. Sundaram and Q. Niu, *Physical Review B* **59**, 14915 (1999).

[60] D. Xiao, Y. Yao, Z. Fang, and Q. Niu, *Physical review letters* **97**, 026603 (2006).

[61] D. Ceresoli, T. Thonhauser, D. Vanderbilt, and R. Resta, *Physical Review B* **74**, 024408 (2006).

[62] T. Thonhauser, D. Ceresoli, D. Vanderbilt, and R. Resta, *Physical review letters* **95**, 137205 (2005).

[63] C. Xiao, Y. Ren, and B. Xiong, *Physical Review B* **103**, 115432 (2021).

[64] L. Dong and Q. Niu, *Physical Review B* **98**, 115162 (2018).

[65] J. Shi, G. Vignale, D. Xiao, and Q. Niu, *Physical review letters* **99**, 197202 (2007).

[66] S. Zhong, J. E. Moore, and I. Souza, *Physical review letters* **116**, 077201 (2016).

[67] Z. Khaidukov, V. Kirilin, and A. Sadofyev, *Physics Letters B* **717**, 447 (2012).

[68] J.-Y. Chen, D. T. Son, M. A. Stephanov, H.-U. Yee, and Y. Yin, *Physical Review Letters* **113**, 182302 (2014).

[69] V. Kirilin, A. Sadofyev, and V. Zakharov, *Physical Review D* **86**, 025021 (2012).

[70] A. Avkhadiev and A. V. Sadofyev, *Physical Review D* **96**, 045015 (2017).

[71] R. Abramchuk, Z. Khaidukov, and M. Zubkov, *Physical Review D* **98**, 076013 (2018).

[72] J.-H. Gao, J.-Y. Pang, and Q. Wang, *Physical Review D* **100**, 016008 (2019).

[73] M.-C. Chang and Q. Niu, *Physical review letters* **75**, 1348 (1995).

[74] M.-C. Chang and Q. Niu, *Physical Review B* **53**, 7010 (1996).

[75] D. Xiao, M.-C. Chang, and Q. Niu, *Reviews of modern physics* **82**, 1959 (2010).

[76] Y. Gao, *Low. Temp. Phys. Lett.* **41**, 0241 (2019).

[77] A. Kamenev, *Field theory of non-equilibrium systems* (Cambridge University Press, 2023).

[78] M. Ogata, *Journal of the Physical Society of Japan* **86**, 044713 (2017).

[79] Z. Rao, H. Li, T. Zhang, S. Tian, C. Li, B. Fu, C. Tang, L. Wang, Z. Li, W. Fan, *et al.*, *Nature* **567**, 496 (2019).

[80] D. Takane, Z. Wang, S. Souma, K. Nakayama, T. Nakamura, H. Oinuma, Y. Nakata, H. Iwasawa, C. Cacho, T. Kim, *et al.*, *Physical review letters* **122**, 076402 (2019).

[81] B. Xu, Z. Fang, M.-Á. Sánchez-Martínez, J. W. Venderbos, Z. Ni, T. Qiu, K. Manna, K. Wang, J. Paglione, C. Bernhard, *et al.*, *Proceedings of the National Academy of Sciences* **117**, 27104 (2020).

SUPPLEMENTAL MATERIAL FOR CHIRAL KINEMATIC THEORY AND CONVERSE VORTICAL EFFECTS

In this paper, we investigate the response of fermions to a space-time-dependent velocity field. We commence with a derivation of the perturbation induced by this velocity field. For this purpose, we consider a system described by the Lagrangian:

$$L_0 = i\partial_t - H_0, \quad (12)$$

where H_0 denotes Hamiltonian. Under a space translation generated by the momentum operator $\hat{\mathbf{p}}$, the Lagrangian L_0 is transformed to L which can be expressed as:

$$L = e^{i\hat{\mathbf{p}} \cdot \mathbf{x}} L_0 e^{-i\hat{\mathbf{p}} \cdot \mathbf{x}} = e^{i\hat{\mathbf{p}} \cdot \mathbf{x}} (i\partial_t - H_0) e^{-i\hat{\mathbf{p}} \cdot \mathbf{x}} = i\partial_t - H_0 + \hat{\mathbf{p}} \cdot \partial_t \mathbf{x} = i\partial_t - (H_0 - \hat{\mathbf{p}} \cdot \mathbf{v}), \quad (13)$$

therefore, the effective Hamiltonian of the system driven by a velocity can be expressed as $H \equiv H_0 + H_1 = H_0 - \hat{\mathbf{p}} \cdot \mathbf{v}$.

APPENDIX A : EQUATIONS OF SEMICLASSICAL MOTION

In this section, we investigate the semiclassical equation of motion using the semiclassical wave-packet dynamics method [59]. We consider a slowly perturbed system described by a Hamiltonian $H(\hat{\mathbf{x}}, \hat{\mathbf{p}}, \mathbf{R}(\hat{\mathbf{x}}, t))$, where $\mathbf{R}(\hat{\mathbf{x}}, t)$ represents a set of modulation functions characterizing the perturbations. Our approach involves examining a wave packet centered at \mathbf{r} and a given time t , with its spatial extent being significantly smaller than the length scale of the perturbations. Under these conditions, we can approximate the Hamiltonian as follows:

$$H(\hat{\mathbf{x}}, \hat{\mathbf{p}}, \mathbf{R}(\hat{\mathbf{x}}, t)) \approx H_c + \frac{1}{2} \left[(\hat{\mathbf{x}} - \mathbf{r}) \frac{\partial H_c}{\partial \mathbf{r}} + \frac{\partial H_c}{\partial \mathbf{r}} (\hat{\mathbf{x}} - \mathbf{r}) \right]. \quad (14)$$

Here, H_c is the local Hamiltonian defined as $H_c \equiv H(\mathbf{r}, \hat{\mathbf{p}}, \mathbf{R}(\mathbf{r}, t))$, which has the same periodicity as the unperturbed system and possesses Bloch bands with Bloch eigenstates satisfying:

$$H_c |\psi(\mathbf{r}, \mathbf{p}, t)\rangle = E_c(\mathbf{r}, \mathbf{p}, t) |\psi(\mathbf{r}, \mathbf{p}, t)\rangle, \quad (15)$$

where \mathbf{p} and $E_c(\mathbf{r}, \mathbf{p}, t)$ are the Bloch vector and band energy, respectively. For the sake of symbolic simplicity, we suppress the band index. The Bloch eigenstates serve as a basis for the wave packet, represented as $|\Psi\rangle \equiv \int d^3\mathbf{p} a(\mathbf{p}, t) |\psi(\mathbf{r}, \mathbf{p}, t)\rangle$, where $a(\mathbf{p}, t)$ denotes the amplitude. The normalization condition is given by :

$$\langle \Psi | \Psi \rangle = 1 = \int d^3\mathbf{p} |a(\mathbf{p}, t)|^2. \quad (16)$$

The amplitude $a(\mathbf{p}, t)$ is narrow compared to the size of the Brillouin zone and has a mean wave vector $\mathbf{q} = \int d^3\mathbf{p} |a(\mathbf{p}, t)|^2 \mathbf{p}$. The wave-packet energy E , which is the expectation value of the Hamiltonian, can be evaluated up to first order in the perturbation gradients using the linearized Hamiltonian :

$$E(\mathbf{r}, \mathbf{q}, t) = E_c(\mathbf{r}, \mathbf{q}, t) + \frac{i}{2} (\langle \partial_{\mathbf{r}} u | \cdot [E_c(\mathbf{r}, \mathbf{q}, t) - H_c(\mathbf{r}, \mathbf{q}, t)] | \partial_{\mathbf{q}} u \rangle - c.c.), \quad (17)$$

where $|u(\mathbf{r}, \mathbf{q}, t)\rangle = e^{-i\mathbf{q}\cdot\mathbf{r}} |\psi(\mathbf{r}, \mathbf{q}, t)\rangle$. We can now derive the corresponding Lagrangian from these expressions :

$$L = -E(\mathbf{r}, \mathbf{q}, t) + \mathbf{q} \cdot \partial_t \mathbf{r} + i \partial_t \mathbf{q} \cdot \langle u | \partial_{\mathbf{q}} u \rangle + i \partial_t \mathbf{r} \cdot \langle u | \partial_{\mathbf{r}} u \rangle + i \langle u | \partial_t u \rangle. \quad (18)$$

This Lagrangian allows us to obtain the equations of motion for the wave packet.

Now, let us consider a system subjected to a weak external velocity field. In the continuum, the corresponding local Hamiltonian is given by: $H_c(\mathbf{r}, \mathbf{q}, \mathbf{v}(\mathbf{r}, t)) = H_0(\mathbf{q}) - \mathbf{q} \cdot \mathbf{v}(\mathbf{r}, t)$. For sufficiently weak velocity fields compared to the typical group velocity, we can approximate the Hamiltonian as follows :

$$H_c(\mathbf{r}, \mathbf{q}, \mathbf{v}(\mathbf{r}, t)) \approx H_0(\mathbf{q} + \mathfrak{M} \cdot \mathbf{v}) \quad (19)$$

where the effective mass tensor \mathfrak{M} is given by:

$$-\mathbf{q} \cdot \mathbf{v} = \frac{1}{2} \{ \frac{\partial H_0(\mathbf{q})}{\partial \mathbf{q}}, \mathfrak{M} \cdot \mathbf{v} \} \quad (20)$$

where $\{, \}$ denotes an anticommutative operation. Equation (20) establishes the relationship between \mathfrak{M} and the gradient of the unperturbed Hamiltonian H_0 . For example, in the case of a free electron gas with $H_0(\mathbf{q}) = \frac{\mathbf{q}^2}{2m_e}$, the effective mass tensor is given by $\mathfrak{M} = -m_e I_{3 \times 3}$. Similarly, for a Weyl fermion with the unperturbed Hamiltonian $H_0(\mathbf{q}) = \mathbf{q} \cdot \boldsymbol{\sigma}$, we find that $\mathfrak{M} = -\sigma_z \mathbf{q}$.

After reintroducing the band index, the term $\mathfrak{M} \cdot \mathbf{v}(\mathbf{r}, t)$ can be thought of as an additive "constant" to the crystal momentum \mathbf{q} . By defining $\mathbf{k} \equiv \mathbf{q} + \mathfrak{M}_n(\mathbf{q}) \cdot \mathbf{v}(\mathbf{r}, t)$, where $\mathfrak{M}_n(\mathbf{q}) \approx \mathfrak{M}_n(\mathbf{k})$ since only linear orders in \mathbf{v} are considered in this work, we will suppress the \mathbf{k} -dependence in $\mathfrak{M}_n(\mathbf{k})$ to simplify notation. The Hamiltonian (19) becomes $H_0(\mathbf{k})$, and its eigenstates have the form $|u_n(\mathbf{r}, \mathbf{q}, t)\rangle = |u_n(\mathbf{k})\rangle$, and the eigenvalues are $\epsilon_n(\mathbf{k})$. This results in the following expression:

$$E_n(\mathbf{r}, \mathbf{k}, t) = \epsilon_{n,\mathbf{k}} + \frac{i}{2} (\langle \partial_{\mathbf{r}} u_{n,\mathbf{k}} | \cdot [\epsilon_{n,\mathbf{k}} - H_0(\mathbf{k})] | \partial_{\mathbf{k}} u_{n,\mathbf{k}} \rangle - c.c.), \quad (21)$$

The last term of Eq. (21) can be expressed as:

$$\begin{aligned} \frac{i}{2} (\langle \partial_{\mathbf{r}} u_{n,\mathbf{k}} | \cdot [\epsilon_{n,\mathbf{k}} - H_0(\mathbf{k})] | \partial_{\mathbf{k}} u_{n,\mathbf{k}} \rangle - c.c.) &= \sum_{ij} \frac{i}{2} (\mathfrak{M}_n \cdot \frac{\partial \mathbf{v}_j}{\partial r_i} \langle \partial_{k_j} u_{n,\mathbf{k}} | [\epsilon_{n,\mathbf{k}} - H_0(\mathbf{k})] | \partial_{k_i} u_{n,\mathbf{k}} \rangle - c.c.) \\ &= - \sum_{lijbc} \frac{i}{2} (\mathfrak{M}_n \cdot \epsilon_{lij} \frac{\partial \mathbf{v}_j}{\partial r_i} \epsilon_{lbc} \langle \partial_{k_b} u_{n,\mathbf{k}} | [\epsilon_{n,\mathbf{k}} - H_0(\mathbf{k})] | \partial_{k_c} u_{n,\mathbf{k}} \rangle) \\ &= - \frac{i}{2} \langle \partial_{\mathbf{k}} u_{n,\mathbf{k}} | \times [\epsilon_n(\mathbf{k}) - H_0(\mathbf{k})] | \partial_{\mathbf{k}} u_{n,\mathbf{k}} \rangle \cdot \mathfrak{M}_n \cdot (\nabla \times \mathbf{v}) \end{aligned} \quad (22)$$

Finally, the Eq. (21) can be expressed as follows:

$$\begin{aligned} E_n(\mathbf{r}, \mathbf{k}, t) &= \epsilon_{n,\mathbf{k}} - \frac{i}{2} \langle \partial_{\mathbf{k}} u_{n,\mathbf{k}} | \times [\epsilon_n(\mathbf{k}) - H_0(\mathbf{k})] \partial_{\mathbf{k}} u_{n,\mathbf{k}} \rangle \cdot \mathfrak{M}_n \cdot (\nabla \times \mathbf{v}) \\ &\equiv \epsilon_{n,\mathbf{k}} - 2\mathbf{m}_n^{\text{orb}} \cdot \mathfrak{M}_n \cdot \mathbf{v}, \end{aligned} \quad (23)$$

where $\mathbf{m}_n^{\text{orb}} \equiv \frac{i}{2} \langle \partial_{\mathbf{k}} u_{n,\mathbf{k}} | \times [\epsilon_n(\mathbf{k}) - H_0(\mathbf{k})] \partial_{\mathbf{k}} u_{n,\mathbf{k}} \rangle$ is the orbital magnetic moment of Bloch electrons, $\mathbf{v} \equiv \frac{1}{2} \nabla \times \mathbf{v}$ is the angular velocity. The last three terms in eq. (18) simply become $i\dot{\mathbf{k}} \cdot \langle u_{n,\mathbf{k}} | \partial_{\mathbf{k}} u_{n,\mathbf{k}} \rangle$. Now the Lagrangian can be expressed as:

$$L = - [\epsilon_{n,\mathbf{k}} - 2\mathbf{m}_n^{\text{orb}} \cdot \mathfrak{M}_n \cdot \mathbf{v}] + \mathbf{k} \cdot \dot{\mathbf{r}} - \dot{\mathbf{r}} \cdot \mathfrak{M}_n \cdot \mathbf{v} + i\dot{\mathbf{k}} \cdot \langle u_{n,\mathbf{k}} | \partial_{\mathbf{k}} u_{n,\mathbf{k}} \rangle. \quad (24)$$

This Lagrangian equation is similar to the one in Equation (3.7) of Ref. [59] with \mathbf{x}_c , \mathbf{k}_c , and $e\mathbf{A}(\mathbf{x}_c, t)$ replaced by \mathbf{k} , \mathbf{r} , and $\mathfrak{M}_n \cdot \mathbf{v}$. The equations of semiclassical motion can be derived variationally from the aforementioned Lagrangian, resulting in:

$$\begin{cases} \dot{\mathbf{r}} = \partial_{\mathbf{k}} h_n^0 - \dot{\mathbf{k}} \times \Omega_n \\ \dot{\mathbf{k}} = -\partial_{\mathbf{r}} h_n^0 - 2\dot{\mathbf{r}} \times \mathfrak{M}_n \cdot \mathbf{v}, \end{cases} \quad (25)$$

where $h_n^0 = \epsilon_{n,\mathbf{k}} - 2\mathbf{m}_n^{\text{orb}} \cdot \mathfrak{M}_n \cdot \mathbf{v}$ and the Berry curvature $\Omega_n \equiv i\nabla \times \langle u_{n,\mathbf{k}} | \partial_{\mathbf{k}} u_{n,\mathbf{k}} \rangle$. Noticing that the energy dispersion represents the relative velocity of electrons to the ions[64], and considering that the lattice moves with velocity $-\mathbf{v}$, the left-hand side of the first equation in Eqs. (25) should be replaced by $\dot{\mathbf{r}} + \mathbf{v}$. By incorporating this modification, we obtain the following equations of motion:

$$\begin{cases} \dot{\mathbf{r}} = \partial_{\mathbf{k}} h_n - \dot{\mathbf{k}} \times \Omega_n, \\ \dot{\mathbf{k}} = -\partial_{\mathbf{r}} h_n - \dot{\mathbf{r}} \times 2\mathfrak{M}_n \cdot \mathbf{v}. \end{cases} \quad (26)$$

where $h_n = \epsilon_{n,\mathbf{k}} - \mathbf{k} \cdot \mathbf{v} - 2\mathbf{m}_n^{\text{orb}} \cdot \mathfrak{M}_n \cdot \mathbf{v} \equiv \epsilon_{n,\mathbf{k}} - \mathbf{k} \cdot \mathbf{v} - 2\mathbf{m}_n^{\text{orb}} \cdot \mathfrak{M}_n \cdot \mathbf{v}$.

APPENDIX B : MODIFICATION OF THE PHASE SPACE MEASURE

In this section, we investigate the impact of the equations of motion on the phase space spanned by noncanonical coordinates. In canonical coordinates, denoted as $\eta = (\mathbf{q}, \mathbf{p})$, the Hamilton equations can be expressed as $\dot{\eta}^\alpha \theta_{\alpha\beta} = \partial_\beta h$, where the antisymmetric matrix $\theta \equiv J = (0, 1; -1, 0)$ is known as the symplectic form[77]. This establishes the foundation for understanding the dynamics in canonical coordinates.

For the equations of motion presented in Eq. (26), the corresponding symplectic form exhibits a distinct structure. It can be expressed as:

$$\omega_{\alpha\beta} = \begin{pmatrix} \epsilon_{\alpha\beta\sigma} (2\mathfrak{M}_n \cdot \mathbf{v})^\sigma & \delta_{\alpha\beta} \\ -\delta_{\alpha\beta} & -\epsilon_{\alpha\beta\sigma} \Omega_n^\sigma \end{pmatrix} \quad (27)$$

This modified symplectic form reveals new insights into the equations of motion in noncanonical coordinates. It highlights the influence of the antisymmetric matrix and the additional terms that arise due to the distinct structure of the symplectic form.

In the canonical coordinates $\eta = (\mathbf{q}, \mathbf{p})$, the phase-space volume element is given by $dV = d\mathbf{q} d\mathbf{p}$. However, when changing coordinates to noncanonical coordinates $\eta \rightarrow \zeta = (\mathbf{r}, \mathbf{k})$, the symplectic form undergoes a transformation. Specifically, $J_{\alpha\beta} \rightarrow \theta_{\alpha\beta} = \frac{\partial \eta^\sigma}{\partial \zeta^\alpha} \frac{\partial \eta^\gamma}{\partial \zeta^\beta} J_{\sigma\gamma}$. This transformation of the symplectic form leads to a corresponding transformation in the phase-space volume element.

The volume element in noncanonical coordinates is given by $dV = \sqrt{|\det \theta|} d\mathbf{r} d\mathbf{k} = (1 + 2\Omega_n \cdot \mathfrak{M}_n \cdot \mathbf{v}) d\mathbf{r} d\mathbf{k}$. This expression elucidates the modification to the volume element due to the transformation and emphasizes the role of the additional terms involving the parameters Ω_n and \mathfrak{M}_n .

These results shed light on the structure of the symplectic form in noncanonical coordinates and its impact on the phase-space volume element. Understanding these transformations is vital for comprehending the dynamics and exploring various physical systems with different coordinate choices.

APPENDIX C : KUBO FORMULA FOR ORBITAL MAGNETIC SUSCEPTIBILITY

In this section, we present a derivation of the response function for a clean (disordered) electron fluid in both the static and uniform limit. The calculation is similar to the one that yields the vortical effect[50], which we refer the reader to for a more detailed description. In the continuum, the perturbation induced by the velocity field can be written as: $H_1 \equiv -i\mathbf{v}(\mathbf{r}, t) \cdot \nabla_{\mathbf{r}}$. In the Bloch basis, the perturbation matrix is composed of $\langle u_{m,\mathbf{k}} | \mathbf{k} | u_{n,\mathbf{k}+\mathbf{q}} \rangle \cdot \mathbf{v}(\mathbf{q}, t)$ and $\langle u_{m,\mathbf{k}} | (-i\nabla_{\rho}) | u_{n,\mathbf{k}+\mathbf{q}} \rangle \cdot \mathbf{v}(\mathbf{q}, t)$. The first term arises from the plane wave component of the Bloch function $\psi_{\mathbf{k}}^n(\mathbf{r})$, while the second term is a result of the periodic part of the Bloch function. The details are as follows:

The Bloch wavefunction for the n -th band is generically of the form $\psi_{\mathbf{k}}^n(\mathbf{r}) \equiv \psi_{\mathbf{k}}^n(\mathbf{R} + \rho) = N^{-1/2} e^{i\mathbf{k} \cdot (\mathbf{R} + \rho)} u_{n,\mathbf{k}}(\rho)$, where N is the number of unit cells, \mathbf{R} is a discrete index that labels them, ρ denotes position within a unit cell, and $u_{n,\mathbf{k}}(\rho)$ is periodic in \mathbf{r} with the same periodicity as the underlying Hamiltonian. In this basis,

$$\langle \psi_{\mathbf{k}}^m | -i\mathbf{v}(\mathbf{r}, t) \cdot \nabla_{\mathbf{r}} | \psi_{\mathbf{k}+\mathbf{q}'}^n \rangle = -i \int_{\mathbf{r}} \psi_{\mathbf{k}}^{m*}(\mathbf{r}) \mathbf{v}(\mathbf{r}, t) \cdot \nabla_{\mathbf{r}} \psi_{\mathbf{k}+\mathbf{q}'}^n(\mathbf{r}) \quad (28)$$

Suppose $\mathbf{v}(\mathbf{r}, t) = e^{-i\mathbf{q} \cdot \mathbf{r}} \mathbf{v}(\mathbf{q}, t)$ is monotonic in space. Approximating $\mathbf{r} \sim \mathbf{R}$ and $\nabla_{\mathbf{r}} = \nabla_{\rho}$, the matrix element becomes

$$\begin{aligned} \langle \psi_{\mathbf{k}}^m | -i\mathbf{v}(\mathbf{r}, t) \cdot \nabla_{\mathbf{r}} | \psi_{\mathbf{k}+\mathbf{q}'}^n \rangle &= -\frac{1}{N} \sum_{\mathbf{R}} e^{i(\mathbf{q}' - \mathbf{q}) \cdot \mathbf{R}} \int_{\rho, \rho'} e^{-i\mathbf{k} \cdot \rho + i(\mathbf{k} + \mathbf{q}' - \mathbf{q}) \cdot \rho'} [u_{m,\mathbf{k}}^*(\rho) i\nabla_{\rho} \delta(\rho - \rho') u_{n,\mathbf{k}+\mathbf{q}'}(\rho')] \cdot \mathbf{v}(\mathbf{q}, t) \\ &= \frac{(2\pi)^3}{N} \sum_{\mathbf{K}} \delta(\mathbf{q}' - \mathbf{q} - \mathbf{K}) \left[\int_{\rho} e^{i(\mathbf{q}' - \mathbf{q}) \cdot \rho} u_{m,\mathbf{k}}^*(\rho) (\mathbf{k} - i\nabla_{\rho}) u_{n,\mathbf{k}+\mathbf{q}'}(\rho) \right] \cdot \mathbf{v}(\mathbf{q}, t) \\ &= \frac{(2\pi)^3}{N} \sum_{\mathbf{K}} \delta(\mathbf{q}' - \mathbf{q} - \mathbf{K}) \left[\int_{\rho} e^{i\mathbf{K} \cdot \rho} u_{m,\mathbf{k}}^*(\rho) (\mathbf{k} - i\nabla_{\rho}) u_{n,\mathbf{k}+\mathbf{q}+\mathbf{K}}(\rho) \right] \cdot \mathbf{v}(\mathbf{q}, t) \end{aligned} \quad (29)$$

where \mathbf{K} are reciprocal lattice vectors. Since $u_{n,\mathbf{k}+\mathbf{q}+\mathbf{K}}(\rho) = e^{-i\mathbf{K} \cdot \rho} u_{n,\mathbf{k}+\mathbf{q}}(\rho)$, the equation above can be expressed as follows:

$$\langle \psi_{\mathbf{k}}^m | -i\mathbf{v}(\mathbf{r}, t) \cdot \nabla_{\mathbf{r}} | \psi_{\mathbf{k}+\mathbf{q}'}^n \rangle = (2\pi)^3 \delta(\mathbf{q}' - \mathbf{q}) \left[\int_{\rho} u_{m,\mathbf{k}}^*(\rho) (\mathbf{k} - i\nabla_{\rho}) u_{n,\mathbf{k}+\mathbf{q}}(\rho) \right] \cdot \mathbf{v}(\mathbf{q}, t) \quad (30)$$

Each term in the sum over \mathbf{K} gives the same contribution and cancels the factor of N . Thus, we can safely assume \mathbf{q} and \mathbf{q}' to be within the first Brillouin zone and write

$$\langle \psi_{\mathbf{k}}^m | -i\mathbf{v}(\mathbf{r}, t) \cdot \nabla_{\mathbf{r}} | \psi_{\mathbf{k}+\mathbf{q}'}^n \rangle = (2\pi)^3 \langle u_{m,\mathbf{k}} | (\mathbf{k} - i\nabla_{\rho}) | u_{n,\mathbf{k}+\mathbf{q}} \rangle \cdot \mathbf{v}(\mathbf{q}, t) \equiv (2\pi)^3 \langle u_{m,\mathbf{k}} | \hat{\mathbf{Q}} | u_{n,\mathbf{k}+\mathbf{q}} \rangle \cdot \mathbf{v}(\mathbf{q}, t) \quad (31)$$

These are the matrix elements of the perturbation in the Bloch basis, and they enter into Kubo's formula, giving the orbital magnetization response to an external velocity field.

The orbital magnetization response to an external velocity field is captured by the response function, which can be expressed as a function of the Green's function and current operator :

$$\chi_{ij}^{\text{orb}}(\mathbf{q}, iq_n) = -\frac{1}{2} \epsilon_{i\mu\nu} i\partial_{q_{\mu}} T \sum_{\mathbf{k}} \int_{\nu_n} \text{tr} [j_{\nu}(\mathbf{k} + \mathbf{q}) G_0(\mathbf{k}, i\nu_n) \hat{Q}_j G_0(\mathbf{k} + \mathbf{q}, i\nu_n + iq_n)], \quad (32)$$

Here, $G_0(\mathbf{k}, i\nu_n)$ represents the standard unperturbed Matsubara Green's function, defined as $[i\nu_n - H_0(\mathbf{k}) + i\text{sgn}(\nu_n)/2\tau]^{-1}$, where $H_0(\mathbf{k})$ denotes the unperturbed Hamiltonian. The ν -th component of the current operator is denoted as j_{ν} and is given by $\frac{\partial H_0}{\partial k_{\nu}}$. Furthermore, we introduce $\hat{\mathbf{Q}} \equiv \hat{\mathbf{k}} - i\nabla_{\rho}$, where $i\nabla_{\rho}$ represents the modification arising from the lattice background[50]. In the continuum limit, $\hat{\mathbf{Q}}$ converges to $\hat{\mathbf{k}}$.

Substituting the expression of G_0 into the above equation for the magnetic susceptibility and defining $\mathbf{Q}^{mn} \equiv \langle u_{m,\mathbf{k}} | \hat{\mathbf{Q}} | u_{n,\mathbf{k}+\mathbf{q}} \rangle$, we obtain:

$$\chi_{ij}^{\text{orb}}(\mathbf{q}, iq_n) = -\frac{1}{2} \epsilon_{i\mu\nu} i\partial_{q_{\mu}} T \sum_{\nu_n} \int_{\mathbf{k}} \sum_{n,m} \frac{\langle u_{n,\mathbf{k}+\mathbf{q}} | j_{\nu}(\mathbf{k} + \mathbf{q}) | u_{m,\mathbf{k}} \rangle}{(i\nu_n - \epsilon_{m,\mathbf{k}} + i\frac{\text{sgn}(\nu_n)}{2\tau})} \frac{Q_j^{mn}}{(i\nu_n + iq_n + \epsilon_{n,\mathbf{k}+\mathbf{q}} + i\frac{\text{sgn}(\nu_n+q_n)}{2\tau})}, \quad (33)$$

which can be simplified as :

$$\begin{aligned}\chi_{ij}^{\text{orb}}(\mathbf{q}, \omega) = & -\frac{i}{2}\epsilon_{i\mu\nu}\int\sum_{\mathbf{k}}\sum_{n,m}\left[\partial_{q_\mu}S_{m,n}(\mathbf{k}, \mathbf{q}, iq_n)\right]\langle u_{n,\mathbf{k}+\mathbf{q}}|j_\nu(\mathbf{k}+\mathbf{q})|u_{m,\mathbf{k}}\rangle Q_j^{mn} \\ & -\frac{i}{2}\epsilon_{i\mu\nu}\int\sum_{n,m}S_{m,n}(\mathbf{k}, \mathbf{q}, iq_n)\left[\partial_{q_\mu}\langle u_{n,\mathbf{k}+\mathbf{q}}|j_\nu(\mathbf{k}+\mathbf{q})|u_{m,\mathbf{k}}\rangle Q_j^{mn}\right],\end{aligned}\quad (34)$$

where $|u_{n,\mathbf{k}}\rangle$ and $\epsilon_{n,\mathbf{k}}$ are the Bloch eigenfunction and eigenenergy of the band n , respectively, and the factor

$$S_{m,n}(\mathbf{k}, \mathbf{q}, iq_n) = T\sum_{i\nu_n}\frac{1}{\left(i\nu_n - \epsilon_{m,\mathbf{k}} + i\frac{\text{sgn}(\nu_n)}{2\tau}\right)}\frac{1}{\left(i\nu_n + iq_n - \epsilon_{n,\mathbf{k}+\mathbf{q}} + i\frac{\text{sgn}(\nu_n+q_n)}{2\tau}\right)},\quad (35)$$

Performing the Matsubara summation and the analytical continuum $iq_n \rightarrow \omega + i0^+$, we get

$$S_{m,n}(\mathbf{k}, \mathbf{q}, \omega) = -\int dz \text{Im}\left[\frac{2}{z + \frac{i}{2\tau}}\right]\frac{f(\epsilon_{m,\mathbf{k}} + z) - f(\epsilon_{n,\mathbf{k}+\mathbf{q}} - z)}{z + \epsilon_{m,\mathbf{k}} - \epsilon_{n,\mathbf{k}+\mathbf{q}} + \omega + \frac{i}{2\tau}},\quad (36)$$

At the limit $(\mathbf{q}, \omega) \rightarrow (\mathbf{0}, 0)$, we get:

$$\begin{aligned}\chi_{ij}^{\text{orb}}(\mathbf{0}, 0) = & -\frac{i}{2}\epsilon_{i\mu\nu}\int\sum_{\mathbf{k}}\sum_{n,m}\left[\frac{dS_{m,n}(\mathbf{k}, \mathbf{0}, 0)}{d\epsilon_{n,\mathbf{k}}}\partial_\mu\epsilon_{n,\mathbf{k}}\right]\langle u_{n,\mathbf{k}}|\partial_\nu H_0(\mathbf{k})|u_{m,\mathbf{k}}\rangle Q_j^{mn} \\ & -\frac{i}{2}\epsilon_{i\mu\nu}\int\sum_{\mathbf{k}}\sum_{n,m}S_{m,n}(\mathbf{k}, \mathbf{0}, 0)\left[\langle\partial_\mu u_{n,\mathbf{k}}|\partial_\nu H_0(\mathbf{k})|u_{m,\mathbf{k}}\rangle Q_j^{mn} + \langle u_{n,\mathbf{k}}|\partial_\nu H_0(\mathbf{k})|u_{m,\mathbf{k}}\rangle\langle u_{m,\mathbf{k}}|\hat{Q}_j|\partial_\mu u_{n,\mathbf{k}}\rangle\right],\end{aligned}\quad (37)$$

At zero temperature and to leading order in τ^{-1} , the factor $S_{m,n}(\mathbf{k}, \mathbf{0}, 0) = \frac{\Theta(-\epsilon_{m,\mathbf{k}}) - \Theta(-\epsilon_{n,\mathbf{k}})}{\epsilon_{m,\mathbf{k}} - \epsilon_{n,\mathbf{k}}}$ for $m \neq n$, and $S_{n,n}(\mathbf{k}, \mathbf{0}, 0) = -\delta(\epsilon_{n,\mathbf{k}})$ or 0. Using the relations

$$\langle u_{n,\mathbf{k}}|\partial_\nu H_0(\mathbf{k})|u_{m,\mathbf{k}}\rangle = -(\epsilon_{n,\mathbf{k}} - \epsilon_{m,\mathbf{k}})\langle u_{n,\mathbf{k}}|\partial_\nu u_{m,\mathbf{k}}\rangle + \delta_{n,m}\partial_\nu\epsilon_{n,\mathbf{k}},\quad (38)$$

and

$$\langle u_{n,\mathbf{k}}|\partial_\nu H_0(\mathbf{k})|\partial_\theta u_{m,\mathbf{k}}\rangle = \epsilon_{n,\mathbf{k}}\langle\partial_\nu u_{n,\mathbf{k}}|\partial_\theta u_{m,\mathbf{k}}\rangle - \langle\partial_\nu u_{n,\mathbf{k}}|H_0(\mathbf{k})|\partial_\theta u_{m,\mathbf{k}}\rangle + \partial_\nu\epsilon_{n,\mathbf{k}}\langle u_{n,\mathbf{k}}|\partial_\theta u_{m,\mathbf{k}}\rangle.\quad (39)$$

The first term on the right-hand side of Eq. (37) can be expressed as follows:

$$-\frac{i}{2}\epsilon_{i\mu\nu}\int\sum_{\mathbf{k}}\sum_{n\neq m}[\delta(\epsilon_{m,\mathbf{k}}) + S_{m,n}(\mathbf{k}, \mathbf{0}, 0)]\langle\partial_\mu u_{m,\mathbf{k}}|\partial_\nu\epsilon_{m,\mathbf{k}}|u_{n,\mathbf{k}}\rangle Q_j^{nm},\quad (40)$$

and the second term on the right-hand side of Eq. (37) can be expressed as follows:

$$\begin{aligned}-\frac{i}{2}\epsilon_{i\mu\nu}\int\sum_{\mathbf{k}}\sum_{n\neq m}S_{m,n}(\mathbf{k}, \mathbf{0}, 0)\left[\langle\partial_\mu u_{m,\mathbf{k}}|\partial_\nu H_0(\mathbf{k})|u_{n,\mathbf{k}}\rangle Q_j^{nm} + \langle u_{m,\mathbf{k}}|\partial_\nu H_0(\mathbf{k})|u_{n,\mathbf{k}}\rangle\langle u_{n,\mathbf{k}}|\hat{Q}_j|\partial_\mu u_{m,\mathbf{k}}\rangle\right] \\ -\frac{i}{2}\epsilon_{i\mu\nu}\int\sum_{\mathbf{k}}\sum_nS_{n,n}(\mathbf{k}, \mathbf{0}, 0)[\langle\partial_\mu u_{n,\mathbf{k}}|(\epsilon_{n,\mathbf{k}} - H_0(\mathbf{k}))|\partial_\nu u_{n,\mathbf{k}}\rangle Q_j^{nn}] \\ -\frac{i}{2}\epsilon_{i\mu\nu}\int\sum_{\mathbf{k}}\sum_nS_{n,n}(\mathbf{k}, \mathbf{0}, 0)\partial_\nu\epsilon_{n,\mathbf{k}}[\langle u_{n,\mathbf{k}}|\hat{Q}_j|\partial_\mu u_{n,\mathbf{k}}\rangle + \langle\partial_\mu u_{n,\mathbf{k}}|u_{n,\mathbf{k}}\rangle Q_j^{nn}],\end{aligned}\quad (41)$$

Combining Eq. (40) and Eq. (41), finally, we obtain the expression for the magnetic susceptibility as:

$$\begin{aligned}
\chi_{ij}^{\text{orb}}(\mathbf{0}, 0) = & - \int_{\mathbf{k}} \sum_{n \neq m} S_{m,n}(\mathbf{k}, \mathbf{0}, 0) \mathcal{M}_i^{mn}(\mathbf{k}) Q_j^{nm} \\
& + \frac{1}{2} \epsilon_{i\mu\nu} \int_{\mathbf{k}} \sum_{n \neq m} S_{m,n}(\mathbf{k}, \mathbf{0}, 0) (\epsilon_{m,\mathbf{k}} - \epsilon_{n,\mathbf{k}}) \langle u_{m,\mathbf{k}} | \partial_{\nu} u_{n,\mathbf{k}} \rangle \langle u_{n,\mathbf{k}} | \partial_{\rho_j} | \partial_{\mu} u_{m,\mathbf{k}} \rangle \\
& + \frac{i}{2} \epsilon_{i\mu\nu} \int_{\mathbf{k}} \sum_{n \neq m} [S_{m,n}(\mathbf{k}, \mathbf{0}, 0) (\epsilon_{m,\mathbf{k}} - \epsilon_{n,\mathbf{k}})] [A_{\nu}^{nm}(\mathbf{k}) A_{\mu}^{mn}(\mathbf{k})] k_j \\
& - \frac{i}{2} \epsilon_{i\mu\nu} \int_{\mathbf{k}} \sum_n S_{n,n}(\mathbf{k}, \mathbf{0}, 0) [\langle \partial_{\mu} u_{n,\mathbf{k}} | (\epsilon_{n,\mathbf{k}} - H_0(\mathbf{k})) | \partial_{\nu} u_{n,\mathbf{k}} \rangle Q_j^{nn}] \\
& - \frac{i}{2} \epsilon_{i\mu\nu} \int_{\mathbf{k}} \sum_{n \neq m} \delta(\epsilon_{m,\mathbf{k}}) \langle \partial_{\mu} u_{m,\mathbf{k}} | \partial_{\nu} \epsilon_{m,\mathbf{k}} | u_{n,\mathbf{k}} \rangle Q_j^{nm} \\
& - \frac{i}{2} \epsilon_{i\mu\nu} \int_{\mathbf{k}} \sum_n S_{n,n}(\mathbf{k}, \mathbf{0}, 0) \partial_{\nu} \epsilon_{n,\mathbf{k}} [\langle u_{n,\mathbf{k}} | \hat{Q}_j | \partial_{\mu} u_{n,\mathbf{k}} \rangle + \langle \partial_{\mu} u_{n,\mathbf{k}} | u_{n,\mathbf{k}} \rangle Q_j^{nn}]. \tag{42}
\end{aligned}$$

where \mathcal{M}_i^{mn} represents the inter-band orbital magnetization matrix for the Bloch electrons [78], which takes the following form,

$$\mathcal{M}_i^{mn}(\mathbf{k}) = \frac{i}{2} \epsilon_{i\mu\nu} [\langle \partial_{\mu} u_{m,\mathbf{k}} | (\partial_{\nu} H_0(\mathbf{k}) + \partial_{\nu} \epsilon_{m,\mathbf{k}}) | u_{n,\mathbf{k}} \rangle]. \tag{43}$$

In some limit conditions, such as the nearly-free electron and deep tight-binding limits [50], the term $\langle u_{n,\mathbf{k}} | \partial_{\rho_j} u_{m,\mathbf{k}} \rangle$ is negligible, and Eq. (42) can be further simplified as:

$$\begin{aligned}
\chi_{ij}^{\text{orb}}(\mathbf{0}, 0) = & - \sum_n \frac{i}{2} \int_{\mathbf{k}} S_{n,n}(\mathbf{k}, \mathbf{0}, 0) [\langle \nabla_{\mathbf{k}} u_{n,\mathbf{k}} | \times (\epsilon_{n,\mathbf{k}} - H_0(\mathbf{k})) | \nabla_{\mathbf{k}} u_{n,\mathbf{k}} \rangle]_i k_j \\
& + \frac{i}{2} \epsilon_{i\mu\nu} \int_{\mathbf{k}} \sum_{n \neq m} [S_{m,n}(\mathbf{k}, \mathbf{0}, 0) (\epsilon_{m,\mathbf{k}} - \epsilon_{n,\mathbf{k}})] [A_{\nu}^{nm}(\mathbf{k}) A_{\mu}^{mn}(\mathbf{k})] k_j. \tag{44}
\end{aligned}$$

The first term accounts for the contribution of the intra-band orbital magnetic moment to the orbital magnetization, while the second term reflects the dependence of the orbital magnetization on the Berry connection of the occupied bands. In the subsequent analysis, we assume the term $\langle u_{n,\mathbf{k}} | \partial_{\rho_j} u_{n,\mathbf{k}} \rangle$ is negligible and thoroughly examine the magnetic susceptibility under different limits, with a specific emphasis on the zero-temperature.

Static limit ($\omega \rightarrow 0$ before $\mathbf{q} \rightarrow \mathbf{0}$)

In the static limit, the factor $S_{m,n}$ can be written as [50]:

$$S_{n,n}(\mathbf{k}, \mathbf{q} \rightarrow \mathbf{0}, 0) = \begin{cases} -\delta(\epsilon_{n,\mathbf{k}}) & |\nabla_{\mathbf{k}} \epsilon_{n,\mathbf{k}} \cdot \mathbf{q} \tau| \gg 1, \\ \frac{1}{\pi} \text{Im} \left[\frac{1}{\epsilon_{n,\mathbf{k}} + \frac{i}{2\tau}} \right] & |\nabla_{\mathbf{k}} \epsilon_{n,\mathbf{k}} \cdot \mathbf{q} \tau| \ll 1, \end{cases} \tag{45}$$

$$S_{m,n}(\mathbf{k}, \mathbf{q} \rightarrow \mathbf{0}, 0) \approx \frac{\Theta(-\epsilon_{m,\mathbf{k}}) - \Theta(-\epsilon_{n,\mathbf{k}})}{\epsilon_{m,\mathbf{k}} - \epsilon_{n,\mathbf{k}}} \text{ for } m \neq n. \tag{46}$$

where τ^{-1} quantifies the strength of disorder. By substituting this expression for factor $S_{m,n}$ into the Eq. (42), and considering the leading order of τ^{-1} , we obtain

$$\begin{aligned}
\chi_{ij}^{\text{orb}}(\mathbf{k}, \mathbf{q} \rightarrow \mathbf{0}, 0) = & \sum_n \int_{\mathbf{k}} \delta(\epsilon_{n,\mathbf{k}}) m_i^{\text{orb}} k_j + \sum_n \int_{\mathbf{k}} \Theta(-\epsilon_{n,\mathbf{k}}) \Omega_n^i k_j \\
& \text{for } |\nabla_{\mathbf{k}} \epsilon_{n,\mathbf{k}} \cdot \mathbf{q} \tau| \gg 1, \tag{47}
\end{aligned}$$

$$\chi_{ij}^{\text{orb}}(\mathbf{k}, \mathbf{q} \rightarrow \mathbf{0}, 0) = \sum_n \int_{\mathbf{k}} \delta(\epsilon_{n,\mathbf{k}}) m_i^{\text{orb}} k_j + \sum_n \int_{\mathbf{k}} \Theta(-\epsilon_{n,\mathbf{k}}) \Omega_n^i k_j$$

for $|\nabla_{\mathbf{k}} \epsilon_{n,\mathbf{k}} \cdot \mathbf{q} \tau| \ll 1$.

(48)

where $m_i^{\text{orb}} \equiv \frac{i}{2} [\langle \nabla_{\mathbf{k}} u_{n,\mathbf{k}} | \times (\epsilon_{n,\mathbf{k}} - H_0(\mathbf{k})) | \nabla_{\mathbf{k}} u_{n,\mathbf{k}} \rangle]_i$ denotes the α th component of the orbital moment, and Ω_n^α is the α th component of the Berry curvature $\boldsymbol{\Omega}_n \equiv \nabla_{\mathbf{k}} \times \mathbf{A}_n$ of n th band.

Uniform limit ($\mathbf{q} \rightarrow \mathbf{0}$ before $\omega \rightarrow 0$)

In the uniform limit, the factor $S_{m,n}$ can be written as:

$$S_{n,n}(\mathbf{k}, \mathbf{0}, \omega \rightarrow 0) = \begin{cases} 0 & |\omega\tau| \gg 1, \\ \frac{1}{\pi} \text{Im} \left[\frac{1}{\epsilon_{n,\mathbf{k}} + \frac{i}{2\tau}} \right] & |\omega\tau| \ll 1, \end{cases}$$
(49)

$$S_{m,n}(\mathbf{k}, \mathbf{0}, \omega \rightarrow 0) \approx \frac{\Theta(-\epsilon_{m,\mathbf{k}}) - \Theta(-\epsilon_{n,\mathbf{k}})}{\epsilon_{m,\mathbf{k}} - \epsilon_{n,\mathbf{k}}} \text{ for } m \neq n.$$
(50)

the factor $S_{m,n}$ is the same as in the static limit for the disorder case, however, the intra-band term $S_{n,n} = 0$ in the clean case. Finally, we obtain the susceptibility in uniform limit for clean and disorder case which is given by:

$$\chi_{ij}^{\text{orb}}(\mathbf{k}, \mathbf{0}, \omega \rightarrow 0) = \sum_n \int_{\mathbf{k}} \Theta(-\epsilon_{n,\mathbf{k}}) \Omega_{n,i} k_j, \quad \text{for } |\omega\tau| \gg 1,$$
(51)

$$\chi_{ij}^{\text{orb}}(\mathbf{k}, \mathbf{0}, \omega \rightarrow 0) = \sum_n \int_{\mathbf{k}} \delta(\epsilon_{n,\mathbf{k}}) m_i^{\text{orb}} k_j + \sum_n \int_{\mathbf{k}} \Theta(-\epsilon_{n,\mathbf{k}}) \Omega_{n,i} k_j$$

for $|\omega\tau| \ll 1$.

(52)